JOURNAL OF Materials CHEMISTRY

Discotic liquid crystals of transition metal complexes, Part 30:† spontaneous uniform homeotropic alignment of octakis(dialkoxyphenoxy)phthalocyaninatocopper(II) complexes‡

Kazuaki Hatsusaka, Kazuchika Ohta,* Iwao Yamamoto and Hirofusa Shirai

Department of Functional Polymer Science, Faculty of Textile Science and Technology, Shinshu University, 386-8567 Ueda, Japan. E-mail: ko52517@giptc.shinshu-u.ac.jp

Received 1st June 2000, Accepted 9th October 2000
First published as an Advance Article on the web 27th November 2000

Six novel octakis(dialkoxyphenoxy)phthalocyaninatocopper(II) complexes (abbreviated as $[(C_nO)_2PhO]_8PcCu$ ($n=9$–14)) have been synthesized. It was found that these derivatives exhibit rich mesophases; Col_h, Col_{r1}, Col_{r2}, Col_{r3}, Col_{tet} and Cub phases. These mesophases were characterized by microscopic observation, DSC measurements and temperature-dependent X-ray diffraction measurements. Temperature-dependent electronic spectra for the thin films of these complexes revealed that roof-top-shaped dimers in the column gradually change into cofacial dimers as the temperature is increased from rt to their clearing points. Furthermore, the phthalocyanine derivatives for $n=11$–14 exhibited spontaneous uniform homeotropic alignment for the Col_{tet} mesophase, which is the first example in discotic liquid crystalline phthalocyanine compounds.

I. Introduction

Discotic liquid crystals are expected to have applications as excellent organic conductors because they have one-dimensional columnar arrays.[2] Generally, liquid crystals are so flexible that they can be spread uniformly on a plate and between two plates. This "large area uniformity" is favorable for electronic devices.[3] Nevertheless, charge-carrier mobilities in the liquid crystalline systems are still slower than those in organic single crystals. On the other hand, it is very difficult to prepare single organic crystals large enough to be used for electronic devices, because they tend to form polycrystalline multidomains. However, flexible discotic liquid crystals may form monodomains in which the disk-like molecules pile up to form one-dimensional arrays, which would be expected to show high conductivity.[4] Hence, the alignment of discotic liquid crystals becomes a crucial point for high conductivity. Two typical alignments of discotic liquid crystals are well-known as homeotropic and homogeneous alignments: in the former the disks lie on a plate horizontally and in the latter the disks stand on a plate perpendicularly. Homeotropic alignment in columnar mesophases can provide an efficient path for electrons and holes along the columnar axis, which is favorable for high conductivity. However, even if discotic liquid crystals exhibit such homeotropic alignment, there are still some problems. Most of the homeotropic alignments contain domain boundaries and disclinations, as shown in a photomicrograph in Fig. 1.[5] Hence, it is very difficult to achieve perfect homeotropic alignment over a large area. To date, few discotic liquid crystals exhibit perfect homeotropic alignment without domain boundaries and disclinations.

Recently, it was revealed from conductivity measurements by TOF methods that a perfectly homeotropically aligned triphenylene derivative **2** (Fig. 2) shows very fast charge-carrier mobilities.[4] It is essential for the conductivity measurements by time of flight (TOF) methods that discotic compounds between two transparent electrodes should show "large area uniformity". Therefore, it is desirable for the investigation and practical usage to develop discotic compounds exhibiting perfect homeotropic alignment over large areas without domain boundaries and disclinations.

As mentioned above, discotic liquid crystals form columnar structures. The high viscosity of columnar mesophases may be attributable to both two-dimensional ordering of columns and the large molecular area contacting with neighbouring disk-like molecules. The high viscosity may cause the easy formation of multidomains. On the other hand, triphenylene derivatives **3** (Fig. 2) which are peripherally substituted by a benzoate ester as a sterically hindering group exhibit a discotic nematic (N_D) mesophase and uniform (monodomain) alignment.[6] Accordingly, the lower viscosity resulting from the introduction of

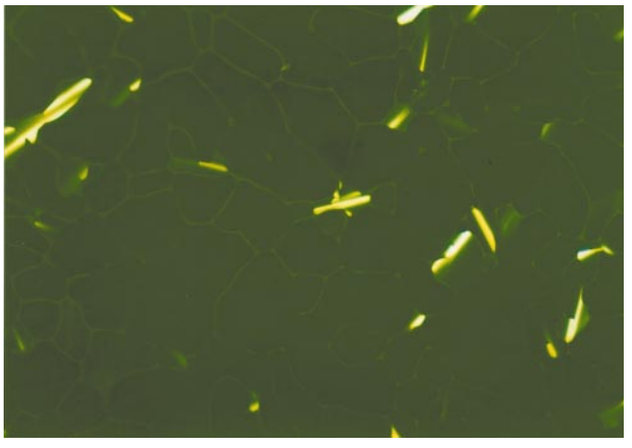

Fig. 1 Photomicrograph of a defective homeotropic alignment of bis[octakis(dodecyloxy)phthalocyaninato]lutetium(III) (**1** in Fig. 2) at 180.0 °C (ref. 5).

†Part 29: Ref. 1
‡Elemental analysis, reprecipitation solvents, yields, and electronic spectral data for $[(C_nO_2)PhO]_8PcCu$ are available as supplementary data. For direct electronic access see http://www.rsc.org/suppdata/jm/b0/b004406g/

DOI: 10.1039/b004406g

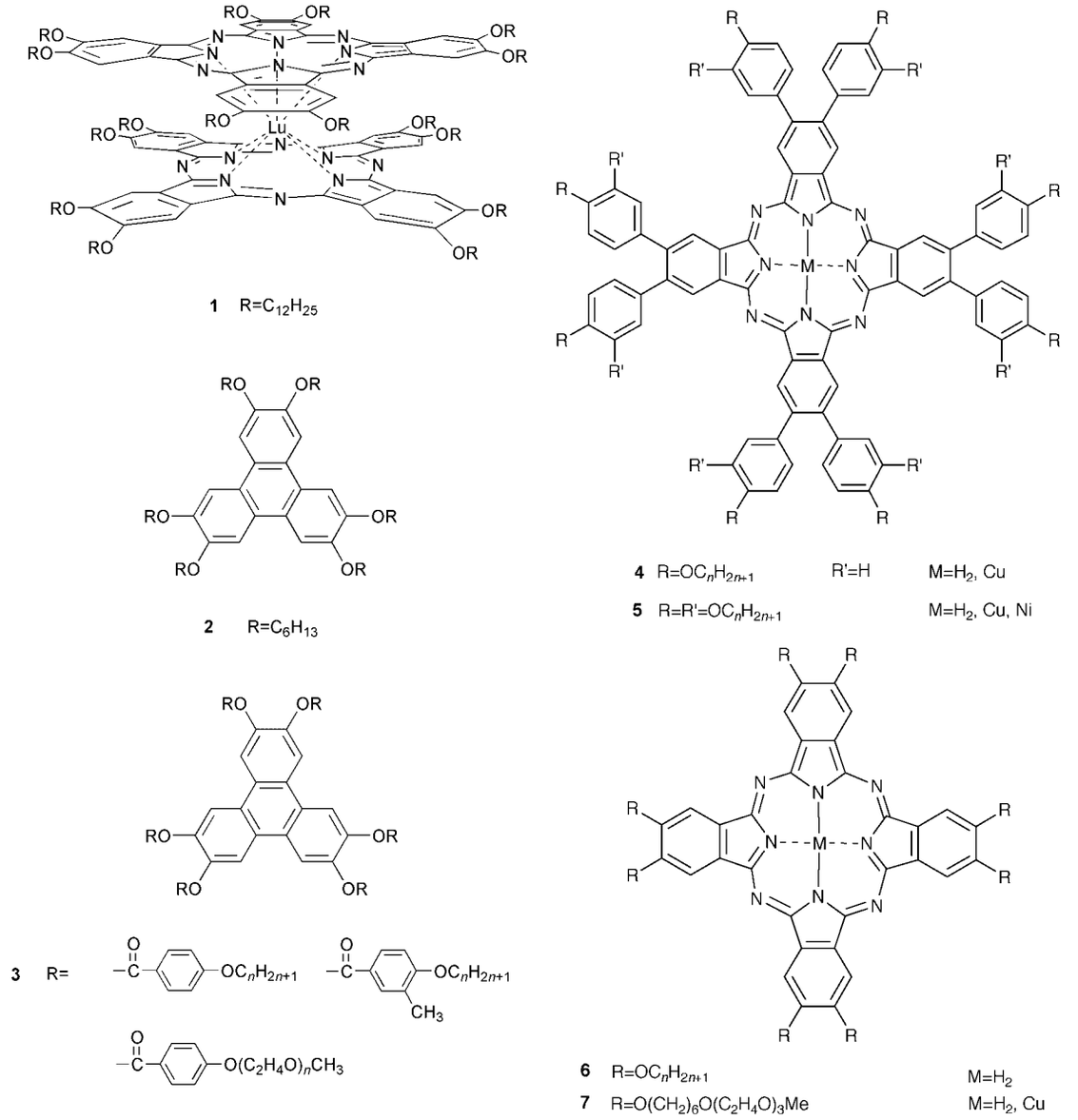

Fig. 2 Formulae of discotic liquid crystalline phthalocyanine and triphenylene derivatives.

sterically hindering groups may more easily achieve a uniform alignment even in columnar mesophases. However, phthalocyanine derivatives **4** and **5** (Fig. 2) which are directly substituted by phenyl groups providing steric hindrance do not show monodomains because of their still high viscosity.[7,8] Octa-*n*-alkoxyphthalocyanine and octa[oligo(ethylene oxide)]alkoxyphthalocyanine derivatives **6** and **7** (Fig. 2) exhibit a homeotropic alignment.[9–11] Their common molecular structure has oxygen atoms between the phthalocyanine core and long chains. Moreover, the above-mentioned triphenylene derivatives **2** and **3** exhibiting monodomains with homeotropic alignment[4,6] also have oxygen atoms intervening between the core and long chains. Hence, we can deduce from these examples that oxygen atoms bonded to a central core may be essential to the homeotropic alignment. In order to achieve such a monodomain with homeotropic alignment, we have synthesized phthalocyanine derivatives **8** (Scheme 1) in which oxygen atoms intervene between the phthalocyanine core and peripheral phenyl groups to decrease the viscosity. According to our expectation, the phthalocyanine derivatives **8** exhibit a spontaneous perfect homeotropic alignment without domain boundaries and disclinations for the first time in phthalocyanine compounds.

Hence, we wish to report here the synthesis of these novel phthalocyanines (**8a**–**f** in Scheme 1) and their interesting physical properties.

II. Experimental

II-1. Synthesis

Synthetic route of this work is shown in Scheme 1. The starting material **9** was commercially available (Tokyo Kasei). The synthesis of 3,4-dialkoxybenzaldehyde **10** was carried out followed by the method of Nguyen *et al.*[12] The 3,4-dialkoxyphenol **11** derivatives could be prepared by the method of van Nostrum *et al.*[13] The 4,5-bis(3,4-dialkoxyphenoxy)-1,2-dicyanobenzene **12** and 2,3,9,10,16,17,23,24-octakis(3,4-dialkoxyphenoxy)phthalocyaninatocopper(II) **8a**–**f** derivatives were prepared by the method of Wöhrle *et al.*[14] The detailed procedures for a representative compound **8d** are described as follows.

3,4-Bis(dodecyloxy)benzaldehyde (10d). 3,4-Dihydroxybenzaldehyde **9d** (5.18 g, 37.5 mmol) and dodecyl bromide (19.8 ml, 82.5 mmol) were dissolved in dry DMF (150 ml). Potassium carbonate (37.3 g, 270 mmol) was added to the

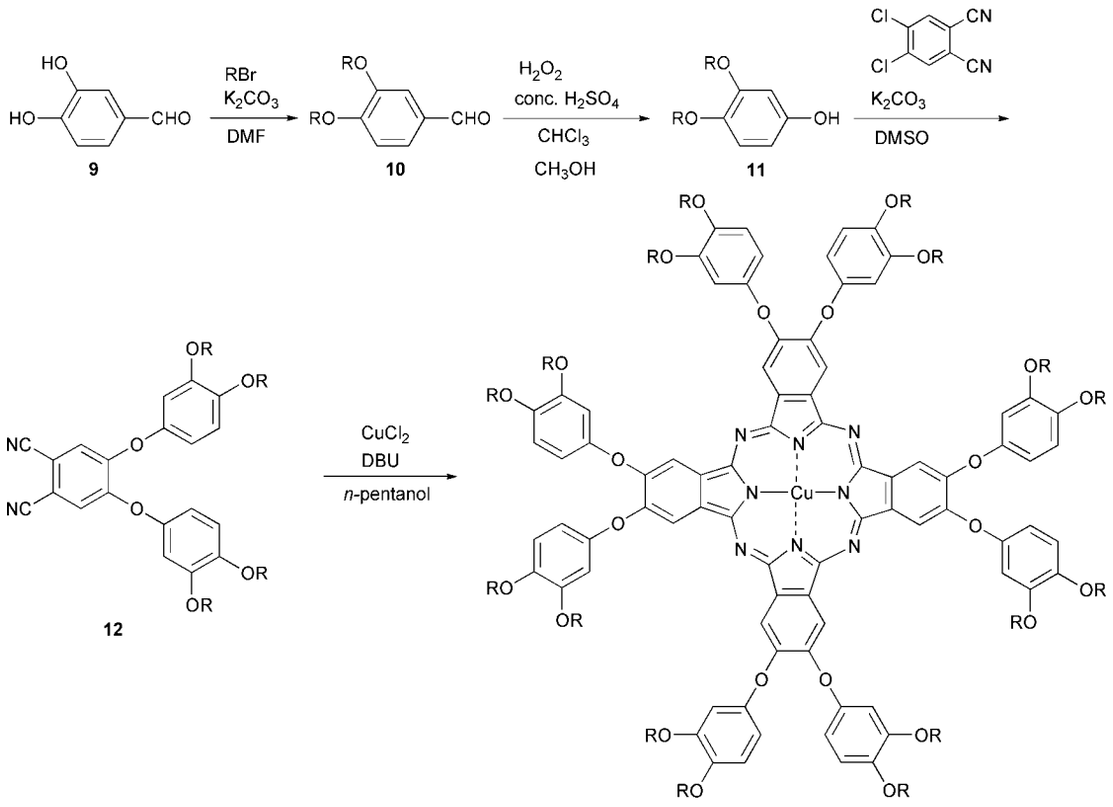

8 $[(C_nO)_2PhO]_8PcCu$

a: R = C_9H_{19} **d:** R = $C_{12}H_{25}$

b: = $C_{10}H_{21}$ **e:** = $C_{13}H_{27}$

c: = $C_{11}H_{23}$ **f:** = $C_{14}H_{29}$

Scheme 1 Synthetic route to the octakis(3,4-dialkoxyphenoxy)phthalocyaninatocopper(II) complexes **8a**–**f**. DMF = *N*,*N*-dimethylformamide; DMSO = dimethyl sulfoxide; DBU = 1,8-diazabicyclo[5.4.0]undec-7-ene.

solution and the mixture was refluxed for 7 hours. The mixture was cooled, extracted with ether and washed with water. Then, the organic layer was dried over Na_2SO_4, filtered and evaporated. After recrystallization from ethanol, the pure compound was obtained as 15.9 g of white crystals. Yield: 89%. Mp = 71.0–71.6 °C.

IR (KBr) 2925, 2850 (CH_2/CH_3), 2750, 1690 (CHO), 1585, 1515 (Ar), 1275, 1240 (Ar–O–C), 865, 805 (Ar–H) cm^{-1}.

^{1}H-NMR ($CDCl_3$: TMS) $\delta = 9.86$ (s, 1H, CHO), 7.41 (dd, $J_1 = 8.96$, $J_2 = 1.80$ Hz, 1H, Ar-H), 7.39 (d, $J = 1.80$ Hz, 1H, Ar-H), 6.94 (d, $J = 9.00$ Hz, 1H, Ar-H), 4.07 (t, $J = 6.25$ Hz, 2H, -CH_2O-), 4.05 (t, $J = 6.25$ Hz, 2H, -CH_2O-), 1.85–1.39 (m, 40H, -$(CH_2)_{10}$-), 0.90 (t, $J = 5.85$ Hz, 6H, -CH_3).

3,4-Bis(dodecyloxy)phenol (11d). The compound **10d** (7.00 g, 14.7 mmol) was dissolved in chloroform (20 ml) and methanol (20 ml). To the solution, a mixture of 3 drops of conc. H_2SO_4 and 30% H_2O_2 (2.22 g, 19.5 mmol) was added. After stirring for 5 hours at room temperature, water was added until the mixture separated into two phases. The organic layer was extracted with chloroform, washed with water, dried over Na_2SO_4, filtered and evaporated. Two recrystallizations from petroleum ether (30–70 °C) gave 3.91 g of pure **11d** as light brown crystals. Yield: 57%. Mp = 82.2–83.1 °C.

IR (KBr) 3290 (OH), 2925, 2850 (CH_2/CH_3), 1605, 1510 (Ar), 1280, 1225 (Ar–O–C), 825, 795 (Ar–H) cm^{-1}.

^{1}H-NMR ($CDCl_3$: TMS) $\delta = 6.75$ (d, $J = 8.57$ Hz, 1H, Ar-H), 6.42 (d, $J = 2.64$ Hz, 1H, Ar-H), 6.28 (dd, $J_1 = 8.46$ Hz, $J_2 = 2.86$ Hz, 1H, Ar-H), 5.11 (br s, 1H, OH), 3.91 (t, $J = 6.59$ Hz, 4H, -CH_2O-), 1.81–1.26 (m, 40H, -$(CH_2)_{10}$-), 0.88 (t, $J = 6.16$ Hz, 6H, -CH_3).

4,5-Bis[3,4-bis(dodecyloxy)phenoxy]-1,2-dicyanobenzene (12d). A mixture of 4,5-dichlorophthalonitrile (0.386 g, 1.96 mmol) and the compound **11d** (2.00 g, 4.32 mmol) in dry DMSO (20 ml) was heated with stirring under the nitrogen atmosphere. To the solution K_2CO_3 was added in 8 portions at intervals of 5 minutes when the reaction solution had reached at 90 °C. The mixture was then stirred for 6 hours at 100 °C. The reaction solution was extracted with chloroform, washed with water, dried over Na_2SO_4, filtered and evaporated. The residue was purified twice by column chromatography (silica gel, $CHCl_3$; $R_f = 0.87$, and then silica gel, $CHCl_3$–*n*-hexane = 7:3; $R_f = 0.61$). The crude product was recrystallized from ethanol (150 ml) twice to afford 1.26 g of white crystals. Yield: 61%. Mp = 79.6, 85.0 °C (two solid polymorphs).

IR (KBr) 2925, 2855 (CH_2/CH_3), 2240 (CN), 1580, 1500 (Ar), 1220, 1070 (Ar–O–C), 870, 800 (Ar–H) cm^{-1}.

^{1}H-NMR ($CDCl_3$: TMS) $\delta = 7.09$ (s, 2H, phenyl protons of the phthalonitrile group), 6.98–6.52 (m, 6H, phenyl protons of the phenoxy group), 4.10–3.90 (m, 8H, -OCH_2-), 1.83–1.27 (m, 80H, -$(CH_2)_{10}$-), 0.93–0.81 (m, 12H, -CH_3).

2,3,9,10,16,17,23,24-Octakis[3,4-bis(dodecyloxy)phenoxy]phthalocyaninatocopper(II) (8d). The compound **12d** (0.200 g, 0.191 mmol) in *n*-pentanol (10 ml) was refluxed in the presence of $CuCl_2$ (0.01 g, 0.07 mmol) and 1,8-diazabicyclo[5.4.0]undec-7-ene (three drops) with stirring under a nitrogen atmosphere for 72 hours. After cooling to room temperature, the reaction solution was extracted with distilled chloroform, washed with water, dried over Na_2SO_4, filtered and evaporated. The residue was washed with hot ethanol (70 ml) for five times, dried and purified by column chromatography (silica gel, $CHCl_3$;

Table 1 Phase transition temperatures and enthalpy changes of the $[(C_nO)_2PhO]_8PcCu$ ($n=9$–14) derivatives

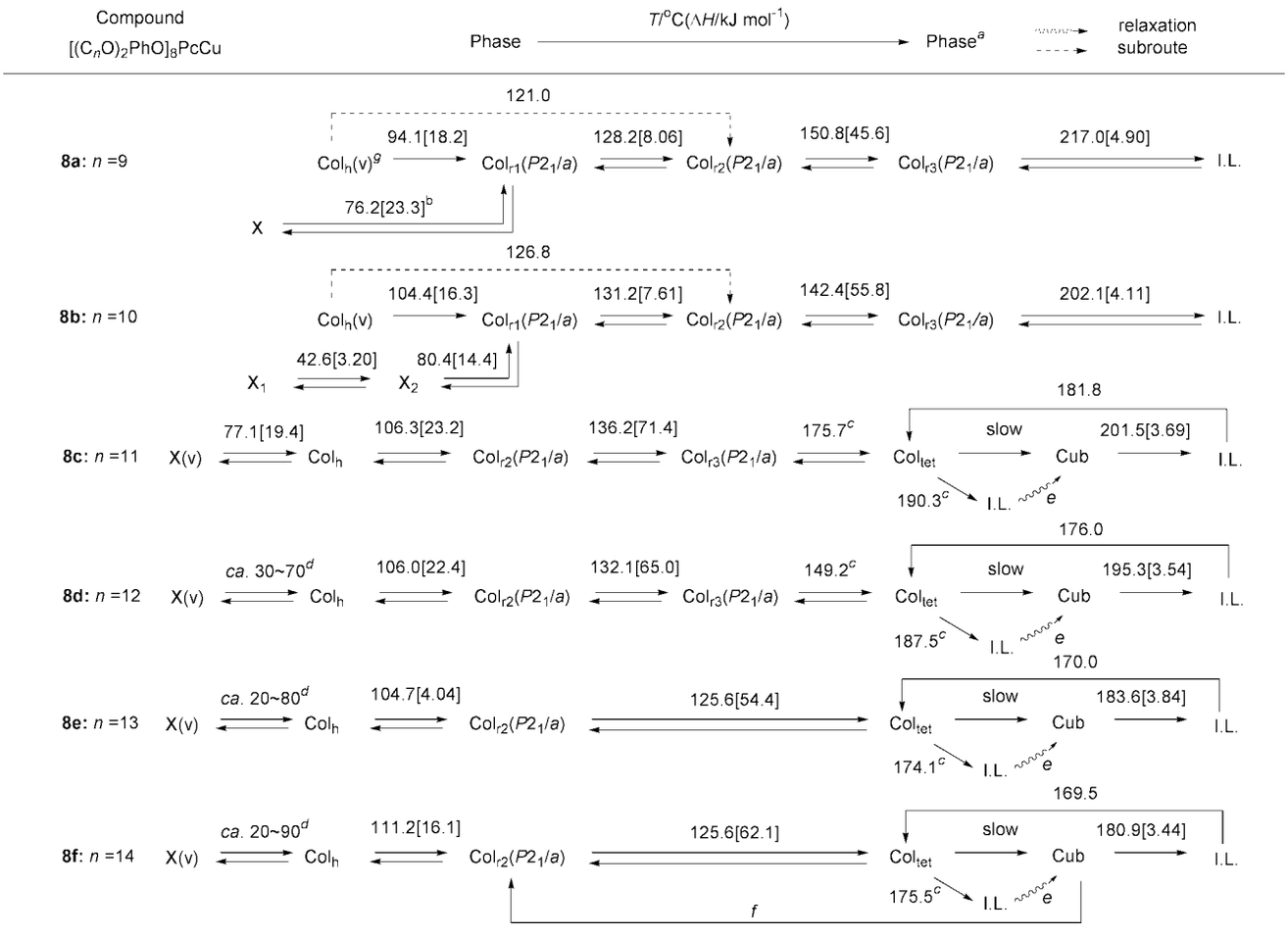

[a]Phase nomenclature: Col_h = hexagonal columnar mesophase, Col_r = rectangular columnar mesophase, Col_{tet} = tetragonal columnar mesophase, X = unidentified mesophase, Cub = cubic mesophase. [b]This X phase could not be obtained in a pure state, so that the biggest enthalpy change listed here is adopted. [c]The enthalpy change was too small to be determined. [d]Very broad endothenmic peak. [e]The I.L. rapidly resolidified into Cub by using seeds of Cub which had resulted from the preceding Col_{tet}–Cub transition. [f]Cub directly transformed into Col_{r2} without proceeding *via* Col_{tet}. (v): Fresh virgin state obtained by recrystallization from solvent.

$R_f=1.00$). To the crude product ethyl acetate (100 ml) was added. It was refluxed to dissolve the residue completely. Into this refluxing solution, ethanol (100 ml) was poured to reprecipitate the product. The reprecipitation was carried out six times to afford 0.129 g of dark green powder. Yield: 63%.

The other derivatives of **10**, **11**, **12** having different alkoxy chain lengths (**a**, **b**, **c**, **e**, **f**) were prepared by the same procedures mentioned above. Purification of the phthalocyanine derivatives **8b**, **d**, **f** was achieved by reprecipitation in a refluxing ethyl acetate solution by adding ethanol. Purification of the derivatives **8a**, **c**, **e** was carried out with reprecipitation from a refluxing *n*-hexane solution by cooling to rt. For the purification, freshly distilled solvents were used. Table S1‡ summarizes the elemental analysis data, reprecipitation solvents and yields for all the $[(C_nO)_2PhO]_8Pc$ derivatives. Table S2‡ lists their electronic spectral data.

II-2. Measurements

The products synthesized here were identified by ^{1}H-NMR (JEOL JNM-FX90A) and IR (Jasco A-100). Further identifications of the present phthalocyanine derivatives **8** were made by elemental analysis (Perkin-Elmer elemental analyzer 2400) and electronic absorption spectroscopy (Hitachi 330 spectrophotometer). The phase transition behaviour of these compounds **8** was observed by using a polarizing microscope (Olympus BH2), equipped with a heating plate controlled by a thermoregulator (Mettler FP80 hot stage, Mettler FP82 Central Processor), and measured by a differential scanning calorimeter (Shimadzu DSC-50). The X-ray diffraction measurements were performed with Cu-Kα radiation (Rigaku Rint) equipped with a hand-made heating plate[15,16] controlled by a thermoregulator. Temperature-dependent electronic absorption spectra were measured by a Hitachi 330 spectrophotometer equipped with a hand-made heating plate[16] controlled by a thermoregulator for the thin films of the phthalocyanine derivatives. These films between two P102 glass plates were prepared by heating above the clearing point (c.p.) and then cooling to rt.

III. Results and discussion

III-1. Mesomorphism

III-1-1. Phase transition behaviour. Phase transition temperatures and enthalpy changes of the $[(C_nO)_2PhO]_8PcCu$ ($n=9$–14: **8a**–**f**) derivatives are summarized in Table 1. These phase transition behaviours were established by microscopic observations, differential scanning calorimetry (DSC) measurements, and temperature-dependent X-ray diffraction studies. All the

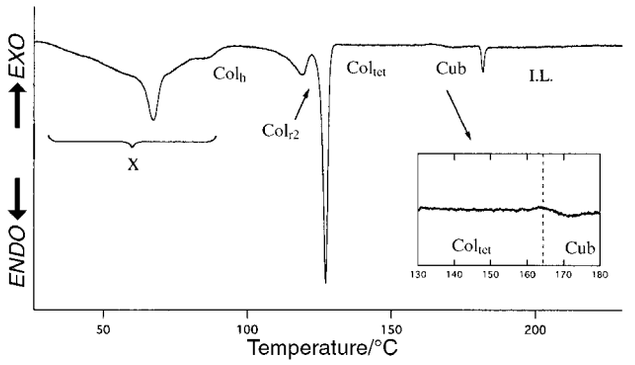

Fig. 3 DSC curve of the $[(C_{14}O)_2PhO]_8PcCu$ derivative for the first heating run at 2.5 °C min^{-1}.

derivatives except for **8a** and **b** gave an unidentified mesophase X as the virgin state by reprecipitation from a solvent at room temperature. Each of the derivatives shows a Col$_h$ mesophase at lower temperatures and at least one Col$_r$ mesophase at higher temperatures: three different Col$_r$ mesophases, Col$_{r1}$, Col$_{r2}$ and Col$_{r3}$, for **8a**, **b**; two Col$_r$ mesophases, Col$_{r2}$ and Col$_{r3}$, for **8c**, **d**; one mesophase, Col$_{r2}$, for **8e**, **f**. As can be seen from Table 1, the Col$_h$ mesophase of **8a**, **b** transformed mainly into Col$_{r1}$ and partially into Col$_{r2}$ (by superheating), and Col$_{r3}$ directly clears into isotropic liquid. It is very surprising to observe the higher symmetry of the Col$_h$ mesophase before the lower symmetry of the Col$_r$ mesophase. This is attributable to a stepwise degradation of roof-top-shaped dimers, as will be described precisely (see later). Recently, we reported that the same phase transition sequence from Col$_h$ to Col$_r$ could be observed for [octakis(3,4-dialkoxyphenyl)tetrapyrazinoporphyrazinato]metal(II) complexes.[17] For **8c**–**f**, a Col$_{tet}$ mesophase and a cubic mesophase, Cub, appear over their Col$_r$ mesophases. When the Col$_r$ mesophase transformed into the Col$_{tet}$ mesophase, spontaneous homeotropic alignment could be observed: the bright mosaic texture of the Col$_r$ mesophase turned into a completely dark area between crossed polarizers for the Col$_{tet}$ mesophase. On further heating, Col$_{tet}$ phase directly transformed into the Cub phase very slowly. Fig. 3 shows a DSC curve of the derivative **8f** at 2.5 °C min^{-1} heating rate. As can be seen from this figure, a slight and gentle change of the base line could be observed at about

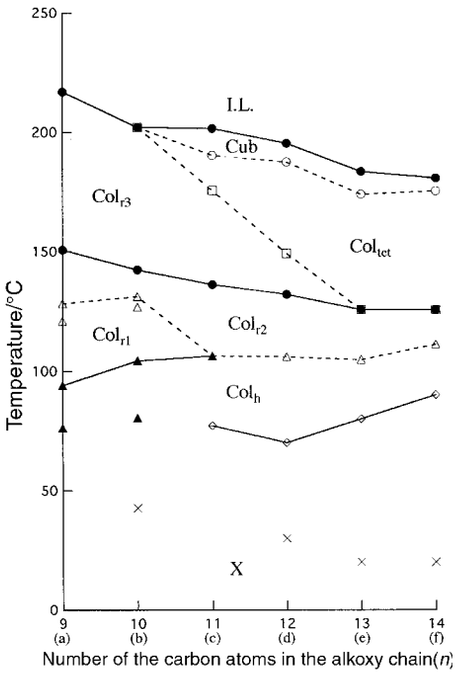

Fig. 4 Phase transition temperature *vs.* n for all the $[(C_nO)_2PhO]_8PcCu$ (n=9–14) derivatives.

165 °C, which may correspond to the phase transition from Col$_{tet}$ to Cub. To confirm this phase transition, temperature-dependent X-ray diffraction patterns of **8f** at 166 °C were recorded at several intervals over 2 hours. At first, the diffraction pattern was almost the same as that for the Col$_{tet}$ phase. It gradually changed into the pattern of the Cub phase. After 2 hours, the pattern became almost the same as that of Cub. Thus, the direct phase transition from Col$_{tet}$ to Cub is very slow. For the microscopic observations at 10 °C min^{-1} heating rate, an additional phase transition from Col$_{tet}$ to I.L. could be repeatedly observed at 175.5 °C. This clearing of Col$_{tet}$ resulted from a superheating of Col$_{tet}$ above the Col$_{tet}$–Cub phase transition temperature at *ca.* 165 °C. The resulting I.L. at 175.5 °C transformed quite fast into a Cub phase by using seeds of Cub which had resulted from the direct phase transition from Col$_{tet}$ to Cub. On further heating, the Cub phase of **8f** completely cleared into I.L. at 180.9 °C. When the I.L. phase above 180.9 °C was cooled, it always transformed into Col$_{tet}$ at 169.5 °C without passing through Cub. The phase transition from I.L. to Cub on cooling could not be detected by microscopic observations and X-ray diffraction studies even when the temperature was held between the two c.p.s of Col$_{tet}$ and Cub over 10 min. This is attributable to the absence of seeds of the Cub phase at the cooling stage. Hence, the I.L. phase can be easily supercooled until Col$_{tet}$ appears at 169.5 °C. When the Cub phase obtained on heating was cooled down instead of elevating temperature to its c.p., the Cub phase transformed into Col$_{r2}$ without passing through the Col$_{tet}$ phase (Route f in Table 1). It was established by X-ray diffraction studies. These direct transformations of both I.L.→Col$_{tet}$ and Cub→Col$_{r2}$ on cooling are attributable to supercooling resulting from the high viscosity of these phases.

All the other phase transitions at lower temperatures were reversible for heating and cooling cycles.

In Fig. 4 all the phase transition temperatures are plotted against number of carbon atoms in the alkoxy chain (n). The line between Col$_{r3}$ and Col$_{tet}$ and the line between Col$_{tet}$ and Cub are very smooth, which supports the existence of Col$_{tet}$ and Cub phases.

III-1-2. Identification of mesophases. These mesophases were identified by temperature-dependent X-ray structural analyses. Three representative derivatives $[(C_nO)_2PhO]_8PcCu$ (n=9, 12, 14) **8a**, **d**, **f** cover all the mesophases appearing in the present homologues, so that only these X-ray data are listed in Table 2.

Col$_h$. Each of the derivatives shows a hexagonal columnar mesophase Col$_h$. For example, compound **8f** at 98 °C gave seven sharp reflections in the small angle region (Table 2), and the spacings are in a ratio of $1:1/\sqrt{3}:1/2:1/\sqrt{7}:1/\sqrt{12}:1/4:1/\sqrt{19}$, which is characteristic of a Col$_h$ mesophase. The mesophases of **8a**, **d** at 68 °C and 94 °C were also established as Col$_h$ in the same way.

Col$_r$. Compound **8a** gave three different rectangular columnar mesophases, Col$_{r1}$, Col$_{r2}$ and Col$_{r3}$. On the other hand, compound **8d** gave two different Colr mesophases, Col$_{r2}$ and Col$_{r3}$. As summarized in Table 2, both of the Col$_{r1}$ and Col$_{r2}$ mesophases could be identified as the same type of mesophase Col$_r$ ($P2_1/a$) from the analysis by using the reciprocal lattice and extinction rules, although the very precise difference between Col$_{r1}$ ($P2_1/a$) and Col$_{r2}$ ($P2_1/a$) could not be clarified at the present time. Since the phase transition from Col$_{r1}$ to Col$_{r2}$ could be repeatedly observed by DSC measurements for **8a**, **b**, these two different Col$_r$ ($P2_1/a$) mesophases surely exist.

Another Col$_{r3}$ mesophase appears for **8a**–**d** (Fig. 4). As shown in Table 2, the Col$_{r3}$ mesophase of **8a** at 156 °C might have two possible symmetries, $P2_1/a$ and $P2m$. Although the Col$_{r3}$ mesophase did not give an additional reflection due to the stacking distance (h) between disks in the column, the number

Table 2 X-Ray data of the representative $[(C_9O)_2PhO]_8PcCu$, $[(C_{12}O)_2PhO]_8PcCu$ and $[(C_{14}O)_2PhO]_8PcCu$ derivatives

Compound (mesophase)	Lattice constants/Å	Spacing/Å		Miller indices (*h k l*)
		Observed	Calculated	
8a: $[(C_9O)_2PhO]_8PcCu$ (Col_h at 68 °C)	$a=36.4$	31.5	31.5	(100)
	$h_1=5.0$	11.9	11.9	(210)
	$Z=1.1$ for $\rho=1.1$[c]	8.78	8.74	(310)
	$h_2=10.0$	6.91	6.88	(410)
	$Z=2.1$ for $\rho=1.1$[c]	*ca.* 4.5	—	[a]
8a: $[(C_9O)_2PhO]_8PcCu$ (Col_{r1} ($P2_1/a$) at 116 °C)	$a=66.2$	33.1	33.1	(200)
	$b=32.9$	29.4	29.4	(110)
	$h_1=4.98$	24.1	23.3	(210)
	$Z=2.0$ for $\rho=1.1$[b]	13.5	13.2	(320)
	$h_2=9.96$	12.4	12.3	(510)
	$Z=4.0$ for $\rho=1.1$[b]	11.3	11.0	(600)
		10.1	9.96	(001): h_2
		9.07	9.08	(710)
		8.22	8.21	(040)
		7.87	7.77	(630)
		6.48	6.44	(250)
		4.98	4.98	(002): h_1
		ca. 4.5	—	[a]
8a: $[(C_9O)_2PhO]_8PcCu$ (Col_{r2} ($P2_1/a$) at 140 °C)	$a=66.2$	33.1	33.1	(200)
	$b=32.4$	29.1	29.1	(110)
	$h_1=5.0$	13.2	13.0	(320)
	$Z=2.0$ for $\rho=1.1$[b]	11.2	11.0	(600)
	$h_2=10.0$	10.2	10.2+10.0	(520) +(001):h_2
	$Z=4.0$ for $\rho=1.1$[b]	9.64	9.69	(330)
		8.15	8.16	(720)
		7.32	7.27	(440)
		6.40	6.44	(150)
		5.92	5.91	(11 10)
		ca. 5.0	5.0	(002):h_1
		ca. 4.5	–	[a]
8a: $[(C_9O)_2PhO]_8PcCu$ (Col_{r3} ($P2_1/a$) at 156 °C)	$a=60.5$	30.2	30.2	(200)
	$b=53.2$	26.6	26.6	(020)
	$h=3.7$[c]	20.0	20.0	(220)
	$Z=2.0$ for $\rho=1.0$[c]	11.5	11.5	(430)
		8.52	8.51	(260)
		ca. 4.6	—	[a]
8a: $[(C_9O)_2PhO]_8PcCu$ (Col_{r3} ($P2m$) at 156 °C)	$a=53.2$	30.2	30.2	(010)
	$b=30.2$	26.6	26.6	(200)
	$h=3.7$[c]	20.0	20.0	(210)
	$Z=1.0$ for $\rho=1.0$[c]	11.5	11.5	(320)
		8.52	8.51	(610)
		ca. 4.6	—	[a]
8d: $[(C_{12}O)_2PhO]_8PcCu$ (Col_h at 94 °C)	$a=41.0$	35.5	35.5	(100)
	$h_1=5.0$[c]	20.5	20.5	(110)
	$Z=1.0$ for $\rho=1.0$[c]	13.4	13.4	(210)
	$h_2=10.0$[c]	10.2	10.2	(220)
	$Z=2.1$ for $\rho=1.0$[c]	*ca.* 4.5	—	[a]
8d: $[(C_{12}O)_2PhO]_8PcCu$ (Col_{r2} ($P2_1/a$) at 120 °C)	$a=73.6$	36.8	36.8	(200)
	$b=36.7$	33.7	32.9	(110)
	$h_1=4.98$	27.5	26.0	(210)
	$Z=1.9$ for $\rho=1.0$[b]	20.0	20.4	(310)
	$h_2=9.96$	14.6	14.6	(320)
	$Z=3.8$ for $\rho=1.0$[b]	13.6	13.7	(510)
		12.9	13.0	(420)
		11.0	11.0	(330)
		9.96	9.96	(001): h_2
		8.86	8.91	(240)
		8.58	8.60	(340)
		7.87	7.87	(540)
		7.36	7.35	(640)
		4.98	4.98	(002) : h_1
		ca. 4.5	—	[a]
8d: $[(C_{12}O)_2PhO]_8PcCu$ (Col_{r3} ($P2_1/a$) at 141 °C)	$a=64.7$	32.3	32.3	(200)
	$b=59.7$	29.9	29.9	(020)
	$h=3.7$[c]	21.9	21.9	(220)
	$Z=2.0$ for $\rho=1.0$[c]	12.3	12.3	(340)
		9.05	9.04	(360)
		ca. 4.6	—	[a]

Table 2 X-Ray data of the representative $[(C_9O)_2PhO]_8PcCu$, $[(C_{12}O)_2PhO]_8PcCu$ and $[(C_{14}O)_2PhO]_8PcCu$ derivatives (*Continued*)

Compound (mesophase)	Lattice constants/Å	Spacing/Å		Miller indices (*h k l*)
		Observed	Calculated	
8d: $[(C_{12}O)_2PhO]_8PcCu$ (Col_{tet} at 165 °C)	$a=43.6$	32.0	30.8	(110)
	$h=3.5^c$	21.8	21.8	(200)
	$Z=0.94$ for $\rho=1.0^c$	12.2	12.1	(320)
		ca. 4.6	—	[a]
8d: $[(C_{12}O)_2PhO]_8PcCu$ (Cub at 192 °C)	$a=150$	35.6	35.4	(333)
	$Z=ca.$ 477 for $\rho=1.0^b$	32.7	32.8	(421)
		30.4	30.6	(422)
		29.4	29.4	(510)
		27.1	27.0	(621)
8f: $[(C_{14}O)_2PhO_8]PcCu$ (Col_h at = 98 °C)	$a=43.2$	37.4	37.4	(100)
	$h_1=5.0^c$	21.6	21.6	(110)
	$Z=1.0$ for $\rho=1.0^c$	18.7	18.7	(200)
	$h_2=10.0^c$	14.2	14.1	(210)
	$Z=2.1$ for $\rho=1.0^c$	10.7	10.8	(220)
		9.26	9.35	(400)
		8.51	8.58	(320)
		ca. 4.6	—	[a]
8f: $[(C_{14}O)_2PhO]_8PcCu$ (Col_{r2} ($P2_1/a$) at 122 °C)	$a=77.8$	38.9	38.9	(200)
	$b=38.8$	36.0	34.7	(110)
	$h_1=5.0^c$	21.4	21.6	(310)
	$Z=1.9$ for $\rho=1.0^c$	18.1	17.4	(410)
	$h_2=10.0^c$	15.3	15.5	(320)
	$Z=3.9$ for $\rho=1.0^c$	11.6	11.6	(330)
		9.24	9.16	(630)
		ca. 4.6	—	[a]
8f: $[(C_{14}O)_2PhO]_8PcCu$ (Col_{tet} at = 147 °C)	$a=45.1$	31.9	31.9	(110)
	$h=3.5^c$	22.7	22.7	(220)
	$Z=0.91$ for $\rho=1.0^c$	9.09	9.02	(340)
		ca. 4.6	—	[a]
8f: $[(C_{14}O)_2PhO]_8PcCu$ (Cub at 179 °C)	$a=149$	37.1	37.3	(400)
	$Z=ca.$ 425 for $\rho=1.0^b$	35.6	35.2	(330)
		34.2	34.3	(331)
		32.2	31.8	(332)
		30.7	30.5	(422)
		28.1	28.7	(511)

[a]Halo of the molten alkoxy chains. [b]Assumed density/g cm^{-3}. [c]When the stacking distance is assumed as $h=X$ (X = 10.0, 5.0, 3.7 Å), the number of molecules in a slice (Z) can be obtained as a number near to an integer ($Z=4$, 2, 1).

of molecules (Z) in a slice was calculated by assuming the stacking distance $h=3.7$ Å and the density $\rho=1.0$ g cm^{-3}.[13] For $P2_1/a$ and $P2m$, the Z values were determined to be 2.0 and 1.0, respectively (Table 2). These Z values are consistent with these two symmetries, $P2_1/a$ and $P2m$. Thereby, it was impossible to conclude the symmetry from these Z values. Then we considered this problem from the tilt angle θ. As illustrated in Fig. 5, the tilt angles for $P2m$ and $P2_1/a$ are thought to be angles θ in Case [A] and Case [B], respectively. For Case [A] ($P2m$), the lattice constant a is equal to the diameter of the disk (see View on *ac* plane), and the lattice constant b is equal to $a\cos\theta$ (see View on *bc* plane). Hence, the tilt angle θ can be calculated from eqn. (1),

$$\theta = \arccos(b/a) \quad (1)$$

where a and b are the lattice constants (Table 2). Hence eqn. (2) is derived.

$$\theta = \arccos(30.2/53.2) \approx 55^\circ \quad (2)$$

On the other hand, the tilt angle θ cannot be calculated in the same manner for Case [B] ($P2_1/a$), because the θ value is not related to the lattice constants for this symmetry. Hence, the angle θ was calculated from the stacking distance. As mentioned above, the stacking distance of compound **8a** at 156 °C can be assumed to be $h=3.7$ Å which is consistent with the Z value calculations. Generally, it is well known that the face-to-face stacking distance for phthalocyanine liquid crystals is 3.4–3.8 Å.[9] Hence, assuming the face-to-face stacking distance to be 3.5 Å for the present Pc compound, the tilt angle θ can be calculated for both Case [A] and [B] from eqn. (3)

$$\theta = \arccos(3.5/3.7) \approx 19^\circ \quad (3)$$

For Case [A] ($P2m$), the tilt angle is 55° from the aforementioned calculation. The results of these two calculations should be equal. Hence, the possibility of $P2m$ symmetry can be excluded. Accordingly, this Col_{r3} mesophase could be identified as Col_r ($P2_1/a$).

Thus, it is very interesting that the present derivative **8a** has three different Col_r ($P2_1/a$) mesophases. The Col_{r3} ($P2_1/a$) mesophase alone does not show stacking order in columns among these three Col_r ($P2_1/a$) mesophases (Table 2), which will be more precisely discussed later.

Col_{tet}. The mesophase of **8f** at 147 °C gave three reflections in the small angle region, and the spacings are in a ratio of $1/\sqrt{2}:1/2:1\sqrt{13}$. This could lead us to conclude that this phase is a tetragonal columnar mesophase Col_{tet}. The Col_{tet} mesophases of **7c–e** were also established in the same way.

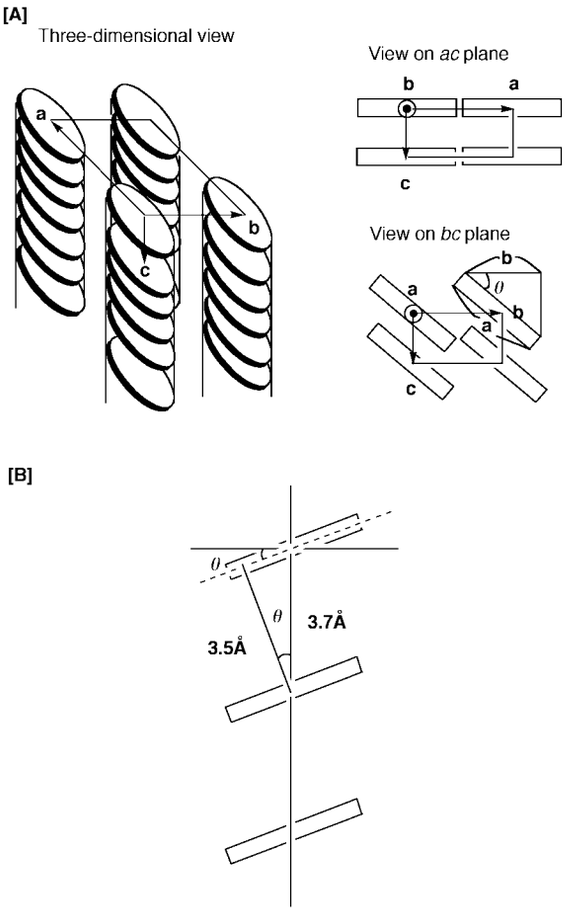

Fig. 5 Tilt angle θ in the rectangular columnar mesophase, Col_{r3}.

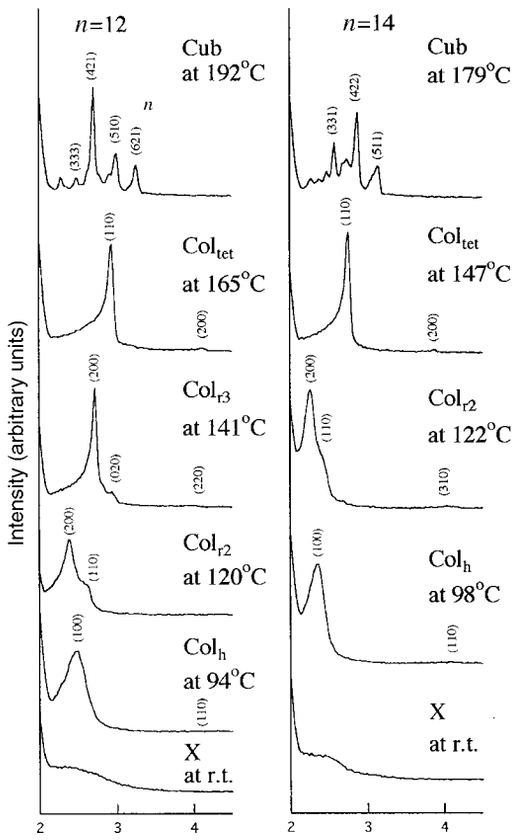

Fig. 6 X-Ray diffraction patterns of the $[(C_nO)_2PhO]_8PcCu$ ($n=12,14$) derivatives in the small angle region ($2\theta=2$–$4.5°$) at various temperatures.

Cub. The highest temperature mesophase for compounds **8c–f** was finally identified as a simple cubic mesophase Cub. Fig. 6 shows the X-ray diffraction patterns of **8d**, **f** for all the phases in the small angle region ($2\theta=2$–$4.5°$) at various temperatures. The patterns of **8d** at 185 °C and **8f** at 176 °C are totally different from all the patterns of general columnar mesophases. As already mentioned above, this mesophase is optically isotropic. If a mesophase is a cubic one, it should be optically isotropic. Hence, the present highest temperature mesophase was analyzed by assuming a cubic phase. All the spacings could be very well indexed to the reflections from a cubic lattice (Table 2). From the extinction rules for cubic lattices, this cubic lattice is a simple cubic one. Thus, it could be identified as a cubic mesophase, Cub.

Each of the highest temperature mesophases of the other derivatives could be identified as the cubic mesophase in the same manner.

III-1-3. Order in columns. *Temperature-dependent X-ray diffraction.* As can be seen from Fig. 7, each of the mesophases of $[(C_9O)_2PhO]_8PcCu$, **8a**, gave a halo at $2\theta=ca.\ 20°$ due to the molten alkoxy chains. The Col_{r1} and Col_{r2} mesophases only gave two additional reflections due to the stacking distance in columns at $h_1\approx5$ Å and $h_2\approx10$ Å. Generally, distance $h_1\approx5$ Å can be observed in Col_{ro} mesophases. Since the h_2 value is almost twice the h_1 value, the molecules in both Col_{r1} and Col_{r2} mesophases partially form dimers to give the additional stacking distance between dimers at $h_2\approx10$ Å. Hence, the Z values could be calculated by using these stacking distances, h_1 and h_2, and assuming the densities $\rho=1.1$ g cm^{-3} for **8a** and $\rho=1.0$ g cm^{-3} for **8d**. As listed in Table 2, the Col_{r1} mesophase of **8a** gave $Z=2.0$ for $h_1=4.98$ Å and $Z=4.0$ for $h=9.96$ Å; the Col_{r2} mesophase of **8a** gave $Z=2.0$ for $h_1=5.0$ Å and $Z=4.0$ for $h_2=10.0$ Å; the Col_{r2} mesophase of **8d** gave $Z=1.9$ for $h_1=4.98$ Å and $Z=3.8$ for $h_2=9.96$ Å. These Z values were thus obtained as integers near to 2 or 4, which are compatible

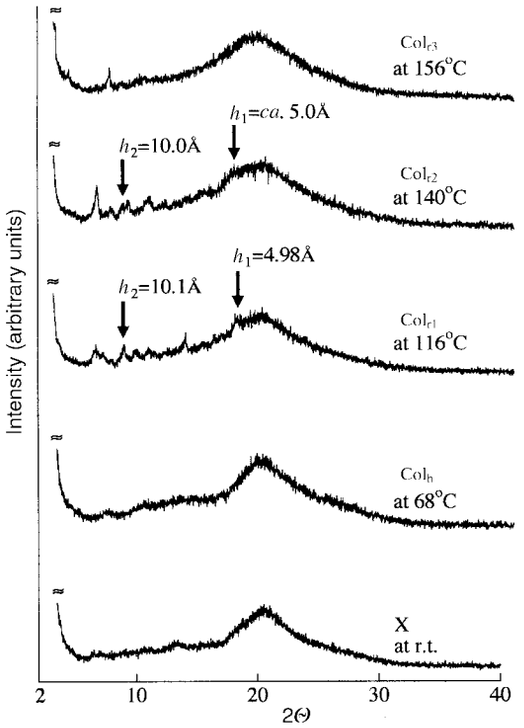

Fig. 7 X-Ray diffraction patterns of the $[(C_9O)_2PhO]_8PcCu$ derivative at various temperatures.

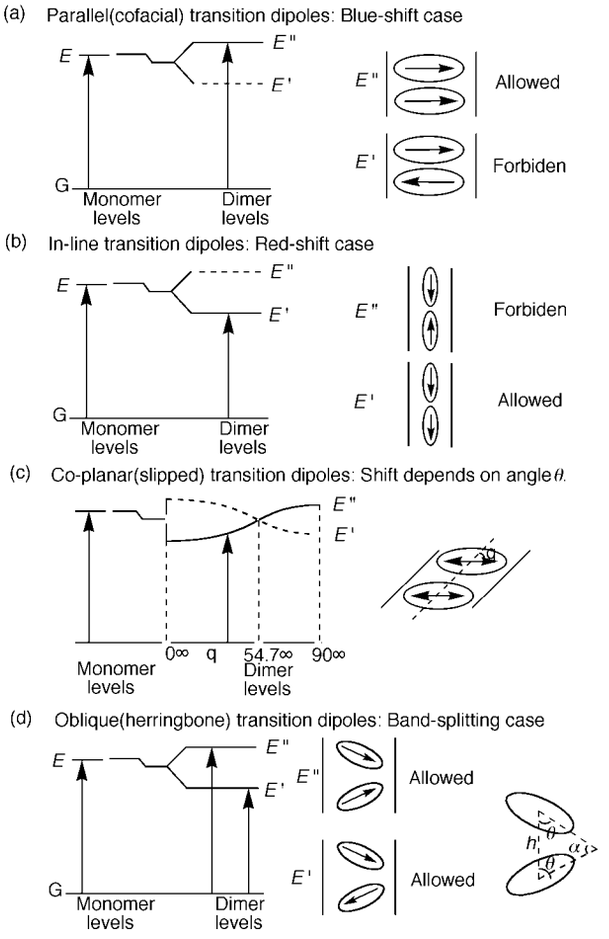

Fig. 8 Exciton energy diagrams for various dimers.

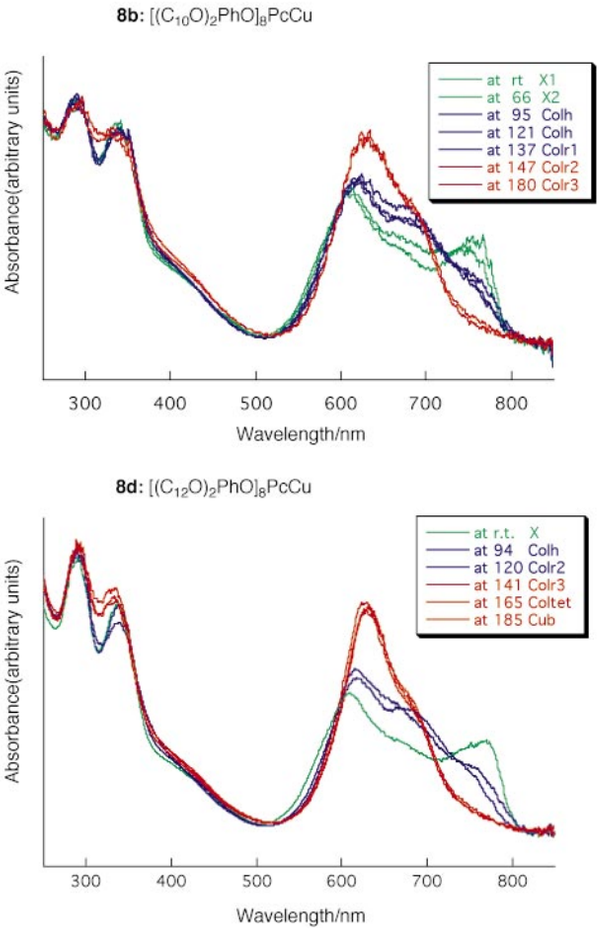

Fig. 9 Temperature-dependent electronic spectra of UV-Vis region of the film of representative $[(C_nO)_2PhO]_8PcCu$ ($n=10,12$) derivatives.

with the theoretical Z values for monomer-stacking and dimer-stacking Col_r ($P2_1/a$) mesophases. Therefore, both values, $h_1=5$ Å and $h_2=10$ Å, can be identified to the stacking distances between monomers and between dimers in columns, respectively.

Temperature-dependent electronic spectra. Kasha *et al.* theoretically explained[18] that interaction between two neighbouring molecules in dimers affects their electronic spectra, as illustrated in Fig. 8. Only the oblique dimers ((d) in Fig. 8) show splitting of the related band. The other types of dimers ((a)–(c) in Fig. 8) do not show the splitting.

Therefore, temperature-dependent electronic spectra of the thin films of compounds **8a**–**f** were recorded. Fig. 9 shows the spectra of the representative derivatives, **8b** and **8d**. As can be seen from this figure, the X phase at rt gave split Q bands at *ca.* 610 nm and 750 nm (green curves), whereas the higher temperature mesophases, Col_{r3}, Col_{tet} and Cub, show an almost single Q band at *ca.* 630 nm (red curves). The intermediate temperature mesophases, Col_h, Col_{r1} and Col_{r2}, gave intermediate spectra (blue curves) which can be formed by superimposition of two previous spectra. The split Q bands of X phase correspond to oblique (roof-top-shaped) dimers shown in Fig. 8(d). On the other hand, the almost single Q bands of Col_{r3}, Col_{tet} and Cub mesophases may correspond to cofacial (face-to-face) or slipped (coplanar) dimers shown in Fig. 8(a) and (c). In-line dimers of Fig. 8(b) can be automatically excluded for the present Pc macrocycles exhibiting columnar mesophases. Therefore, the shape in the intermediate temperature mesophases, Col_h, Col_{r1} and Col_{r2}, may be in an equilibrium between the roof-top-shaped dimers and cofacial (or coplanar) dimers.

The roof-top-shaped dimers are further considered from the angle θ illustrated in Fig. 8(d). In this figure, h, θ, and α represent a distance between molecular centers of the dimer, a base angle and a vertical angle, respectively. From Kasha's rule,[17] the energy gap ΔE of split Q bands is given in eqn. (4)

$$\Delta E = E'' - E' = 2|\mathrm{M}|^2(\cos\alpha + 3\cos^2\theta)/h^3 \quad (4)$$

where M represents the transition moment for the singlet–singlet transition in the monomer, see eqn. (5)

$$\Delta E \propto (\cos\alpha + 3\cos^2\theta) \quad (5)$$

From $\alpha+\theta=180°$, $\alpha=180°-2\theta$ we get eqn. (6)

$$\cos\alpha = \cos(180^\circ - 2\theta) = -\cos 2\theta \quad (6)$$

From eqns. (5) and (6) we can derive eqn. (7)

$$\Delta E \propto (-\cos 2\theta + 3\cos^2\theta) = \cos^2\theta + 1 \quad (7)$$

When $\cos\theta = x$ $(0<\theta<90°)$, $f(x)$ is set as eqn. (8):

$$f(x) = x^2 + 1 (0 < x < 1) \quad (8)$$

From eqn. (7) and (8), ΔE increases with decreasing θ to 90°, and decreases with increasing θ to 90°. In other words, the energy gap between split Q bands becomes narrower as the dimers become more parallel, and finally show a single non-split Q band. As can be seen from Fig. 9, the split Q bands gradually change into a single non-split Q band with increasing temperature. Therefore, this implies that the roof-top-shaped dimers gradually change into the cofacial (or coplanar) dimers.

Taking account for both results of the X-ray diffraction and electronic spectra, the stacking structures in columns of **8a**–**f** are depicted in Fig. 10. In the X phase, the molecules form roof-top-shaped dimers (Fig. 10[C]). On heating these dimers

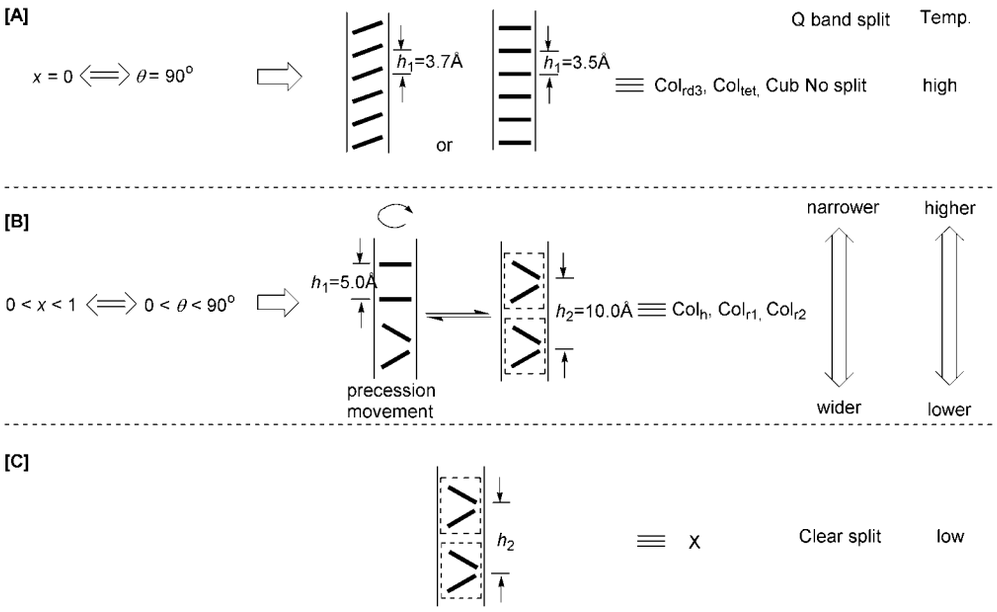

Fig. 10 Relationship of the stacking structure in column to the Q band split and temperature.

begin to freely rotate to show precession movement in the Col_h, Col_{r1} and Col_{r2} mesophases (Fig. 10[B]). In these mesophases, the roof-top-shaped dimers may be partially destroyed by the precession movement, so that an equilibrium between the roof-top-shaped dimers and rotating monomers may exist. Such rotating monomers by precession movement give a monomer stacking distance at 5 Å on the time average. Accordingly, two different stacking distances, h_1 and h_2, can be observed at 5 Å and 10 Å at the same time for the Col_{r1} and Col_{r2} mesophases. On further heating, the roof-top-shaped dimers are totally destroyed into the coplanar or cofacial monomers in the Col_{r3}, Col_{tet} and Cub mesophases (Fig. 10[A]).

The Cub mesophase may maintain a columnar structure. It was revealed from the X-ray diffraction study that the Cub mesophase has a simple cubic lattice having the lattice constant $a = ca.$ 140–160 Å and the number of molecules in a unit cell $Z = ca.$ 440–480 for **8c–f**. It is very unlikely that such disk-like molecules would form a big round ball containing *ca.* 440–480 molecules. For lyotropic cubic mesophases, a 'bicontinuous' aggregated structure is well-known.[19] In this mesophase, branched long columns form a network like a "jungle gym". Probably, the present Cub mesophase forms a similar "bicontinuous" aggregated structure using the long flexible columns. It is noteworthy that this cubic mesophase is the first example in phthalocyanine-based liquid crystals, so far as we know.

III-2. Spontaneous homeotropic alignment for the Col_{tet} mesophase

As can be seen from the photomicrographs in Fig. 11, "uniform (monodomain)" homeotropic alignment without domain boundaries and disclinations could be achieved only for the Col_{tet} mesophase *between* soda-lime or quartz glass plates. It is the first example of spontaneous uniform homeotropic alignment in phthalocyanine-based liquid crystals, so far as we know. "Polydomain" appeared for the Col_{tet} mesophase *on* a soda-lime glass plate and a quartz glass plate, but homeotropic alignment without disclinations could be still achieved even for these free faces.

Such a uniform homeotropic alignment in the Col_{tet} mesophase is attributable to the oxygen atoms and octaphenoxy groups in the present Pc derivatives, **8**.

Although Pc derivatives **5** (Fig. 2) strongly resemble the present Pc derivatives, **8**, they do not show homeotropic alignment. The molecular difference between **5** and **8** consists only of oxygen atoms between the phenyl groups and phthalocyanine core. Hence, the oxygen atoms cause the homeotropic alignment for **8**. It is well known that water molecules adhere onto glass plates in monolayer fashion, which is attributable to coordination of the lone pairs of the oxygen atom in H_2O to the dangling bonds of silicon atoms on glass. Similarly, lone pairs of the phenoxy group in the present phthalocyanine derivatives may coordinate to the dangling bonds of silicon atoms on the surface of glass and/or quartz,

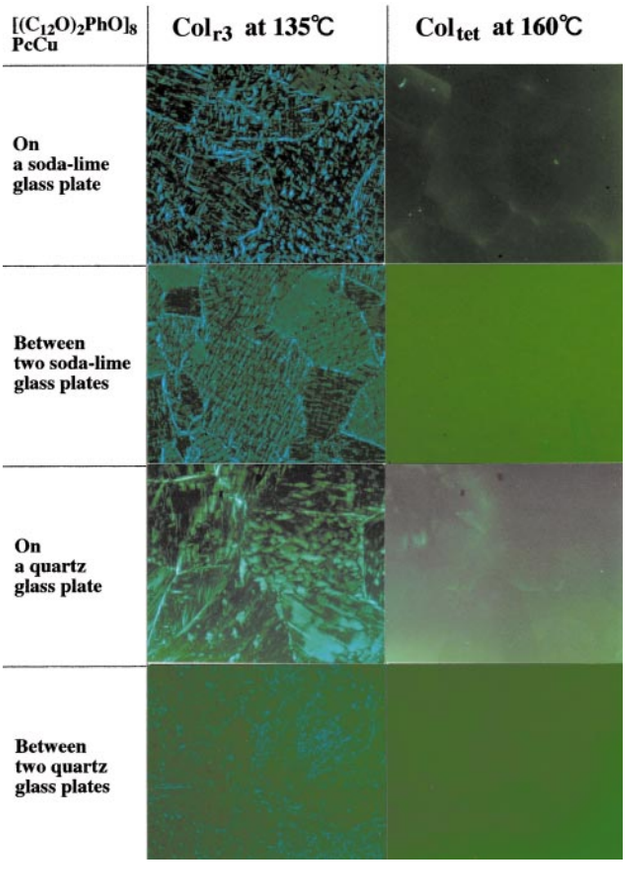

Fig. 11 Polarizing photomicrographs of the $[(C_{12}O)_2PhO]_8PcCu$ for the Col_{r3} and Col_{tet} mesophases at 135 °C and 160 °C, respectively.

like H_2O molecules. The first Pc disk adhered to the surface may trigger the stacking of the disks one after another. Since this is only a speculation from the analogy, further studies are necessary.

Generally, discotic liquid crystals show high viscosity and form multidomains with many domain boundaries. On the other hand, an N_D mesophase of the triphenylene derivatives **3** with low viscosity shows a uniform monodomain with homeotropic alignment. Hence, low viscosity should be necessary to achieve such a uniform monodomain. Since both compounds **3** and **8** have eight phenyl groups in their surroundings, their uniform monodomain is attributed to the steric hindrance of these groups.

IV. Conclusion

Novel phthalocyanine-based liquid crystals, **8a**–**f**, were successfully synthesized. These Pc derivatives show quite rich mesophases; X, Col_h, Col_r (Col_{r1}, Col_{r2}, Col_{r3}), Col_{tet} and Cub. The molecular structure in the columns changes stepwise from roof-top-shaped dimers in the X phase to cofacial or coplanar monomers in the Col_{r3}, Col_{tet} and Cub mesophases: an equilibrium between the roof-top-shaped dimers and the cofacial (coplanar) monomers in columns exists in the intermediate temperature mesophases, Col_h, Col_{r1} and Col_{r2}, and precession movement of the disks gives two different stacking distances, h_1 and h_2, for these mesophases. For the Col_{tet} mesophase, "spontaneous uniform homeotropic alignment" could be observed for the first time in phthalocyanine-based liquid crystals. Moreover, the simple cubic mesophase, Cub, could be obtained for the first time in phthalocyanine-based liquid crystals.

Acknowledgements

This work was partially supported by a Grant-in-Aid for COE Research (10CE2003) and Research (12129205) by the Ministry of Education, Science, Sports and Culture of Japan.

References

1 Part 29: K. Ban, K. Nishizawa, K. Ohta, A. M. van de Craats, J. M. Warman, I. Yamamoto and H. Shirai, *J. Mater. Chem.*, in the press, DOI 10.1039/b003984p.
2 A. M. van de Craats, P. G. Schouten and J. M. Warman, *Ekisho*, 1998, **2**, 12.
3 J. Hanna, *Oyo Butsuri*, 1999, **68**, 26.
4 D. Adam, P. Schuhmacher, J. Simmerer, L. Häussling, K. Siemensmeyer, K. H. Etzbach, H. Ringsdorf and D. Haarer, *Nature*, 1994, **371**, 141.
5 A. M. van de Craats, J. M. Warman, H. Hasebe, R. Naito and K. Ohta, *J. Phys. Chem. B*, 1997, **101**, 9224.
6 K. Kawata, M. Negoro, H. Nishikawa and M. Okazaki, *Ekisho*, 1998, **1**, 45.
7 K. Ohta, T. Watanabe, S. Tanaka, T. Fujimoto, I. Yamamoto, P. Bassoul, N. Kuchanczyk and J. Simon, *Liq. Cryst.*, 1991, **10**, 357.
8 K. Ohta, S. Azumane, T. Watanabe, S. Tsukada and I. Yamamoto, *J. Appl. Organometallic Chem.*, 1996, **10**, 623.
9 J. Simon and P. Bassoul, *Phthalocyanines Properties and Applications*, ed. C. C. Leznoff and A. B. P. Lever, Wiley-VCH, New York, 1995, p. 258; and references cited therein.
10 J. F. Van der Pol, E. Neeleman, J. W. Zwikker, R. J. M. Nolte and W. Drenth, *Liq. Cryst.*, 1989, **6**, 577.
11 J. M. Kroon, R. B. M. Koehorst, M. van Dijk, G. M. Sanders and E. J. R. Sudhölter, *J. Mater. Chem.*, 1997, **7**, 615.
12 H. T. Nguyen, C. Destrade and J. Malthete, *Liq. Cryst.*, 1990, **8**, 797.
13 C. F. van Nostrum, S. J. Picken, P. G. Schouten and R. J. M. Nolte, *J. Am. Chem. Soc.*, 1995, **117**, 9957.
14 D. Wöhrle, M. Eskes, K. Shigehara and A. Yamada, *Synthesis*, 1993, 194.
15 H. Ema, Master Thesis, Shinshu University, Ueda, Japan, 1988, ch. 7.
16 H. Hasebe, Master Thesis, Shinshu University, Ueda, Japan, 1991, ch. 5.
17 K. Ohta, S. Azumane, W. Kawahara, N. Kobayashi and I. Yamamoto, *J. Mater. Chem.*, 1999, **9**, 2313.
18 M. Kasha, H. R. Rawls and M. A. El-Bayoumi, *Pure. Appl. Chem.*, 1965, **11**, 371.
19 C. Fairhurst, S. Fuller, J. Gray, M. C. Holmes and G. J. T. Tiddy, *Handbook of liquid Crystals*, ed. D. Demus, J. Goodby, G. W. Gray, H.-W. Spiess and V. Vill, Wiley-VCH, 1998, vol. 3, ch. VII.